Electronic Supplementary Information

Three dimensional graphene-supported nitrogen-doped carbon nanotube architecture for attenuation of electromagnetic energy

Xiao Zhang,[a,b] Xinci Zhang,[a] Deting Wang,[a] Haoran Yuan,[a] Shen Zhang,[a] Chunling Zhu,[*b] Xitian Zhang[c] and Yujin Chen[*a]

[a] Key Laboratory of In-Fiber Integrated Optics, Ministry of Education and College of Science, Harbin Engineering University, Harbin 150001, China.

[b] College of Chemistry and Chemical Engineering, Harbin Engineering University, Harbin 150001, China.

[c] Key Laboratory for Photonic and Electronic Bandgap Materials, Ministry of Education and School of Physics and Electronic Engineering, Harbin Normal University, Harbin 150025, China.

*Corresponding authors.

Tel.: +086-0451-82519754, Fax: +086-0451-82519754

E-mail addresses: zhuchunling@hrbeu.edu.cn (C. Zhu) or chenyujin@hrbeu.edu.cn (Y. Chen).

Experimental details

Chemicals. Graphene sheets were obtained Nanjing XFNANO Material Tech Co., Ltd. (China). Cobalt nitrate hexahydrate ($Co(NO_3)_2 \cdot 6H_2O$, > 98.5 %) was purchased from Sinopharm Chemical Reagent Co., Ltd (China). Nickel nitrate hexahydrate ($Ni(NO_3)_2 \cdot 6H_2O$, > 98 %) was purchased from Tianjin Guangfu Science and Technology Development Co., Ltd. (China). 2-methylimidazole ($C_4H_6N_2$, > 98 %), dicyanodiamide ($C_2H_4N_4$, > 99 %) and ethanol (C_2H_5OH, > 99.7 %) were purchased from Tianjin Guangfu Fine Chemical Research Institute (China). Methanol (CH_3OH, > 99.9 %) was purchased from Xilong Scientific Co., Ltd. (China). Paraffin was purchased from Yuyang Wax Industry (China). All the chemicals were directly used after purchase without further purification.

Synthesis of G/Co-MOF composites. G/Co-MOF composite was first synthesized through a previously reported method. First, 10 mg graphene is dispersed in 25 mL of methanol sonicated for 30 min aim to ultrasonic uniformity of graphene. 72 mg of cobalt nitrate hexahydrate was added into graphene suspension for solution A. The suspension was sonicated for 20 min, made the Co^{2+} fully contact with graphene. 82 mg of 2-methylimidazolate was dissolved in 15 mL of methanol for solution B, respectively. Then the solution B was added to the solution A under constant stirring with magnetic at 30 min at room temperature. Then the solution was transferred into a 50 mL teflonlined stainless steel autoclave and kept in an oven at 120 °C for 6 hours. The composite was harvested by centrifugation and washed with methanol several times. The product was eventually dried in a vacuum oven at 60 °C for overnight.

Synthesis of G/CoNi-MOF/LDH composites. G/Co$_1$Ni$_1$-MOF/LDH composites were also synthesized with the same method. First, 10 mg of graphene is dispersed in 25 mL of methanol sonicated for 30 min aim to ultrasonic uniformity of graphene. 36 mg of cobalt nitrate hexahydrate and 36 mg of nickel nitrate hexahydrate were added into graphene suspension for solution A. The suspension was sonicated for 20 min, made the Co^{2+} and Ni^{2+} fully contact with graphene. 82 mg of 2-methylimidazolate was dissolved in 15 mL of methanol for solution B, respectively. Then the solution B was added to the solution A under constant stirring with magnetic at 30 min at room temperature. Then the solution was transferred into a 50 mL teflonlined stainless steel autoclave and kept in an oven at 120 °C for 6 hours. The composite was harvested by centrifugation and washed with methanol several times. The product was eventually dried in a vacuum oven at 60 °C for overnight. The G/Co$_3$Ni$_1$-MOF/LDH and G/Co$_1$Ni$_3$-MOF/LDH were synthesized with the same method. (54 mg of cobalt nitrate hexahydrate and 18 mg of nickel nitrate hexahydrate or 18 mg of cobalt nitrate hexahydrate and 54 mg of nickel nitrate hexahydrate were added into graphene suspension for

solution A.)

Synthesis of G/NiNi-LDH composites. G/NiNi-LDH composite was also synthesized with the same method. First, 10 mg graphene is dispersed in 25 mL of methanol sonicated for 30 min aim to ultrasonic uniformity of graphene. 73 mg of nickel nitrate hexahydrate was added into graphene suspension for solution A. The suspension was sonicated for 20 min, made the Ni^{2+} fully contact with graphene. 82 mg of 2-methylimidazolate was dissolved in 15 mL of methanol for solution B, respectively. Then the solution B was added to the solution A under constant stirring with magnetic at 30 min at room temperature. Then the solution was transferred into a 50 mL teflonlined stainless steel autoclave and kept in an oven at 120 °C for 6 hours. The composite was harvested by centrifugation and washed with methanol several times. The product was eventually dried in a vacuum oven at 60 °C for overnight.

Synthesis of G/Co@NCNTA, G/CoNi@NCNTAs and G/Ni@NCNTA composites. 20 mg of samples and 4 g of dicyandiamide (DCD) were transferred into two ceramic boats, respectively. Then put them together in a tube furnace and the powder were heated to 400 °C for 2 h and 700 °C for another 2 h at a speed of 5 °C min^{-1} under a flowing Ar atmosphere. The G/Co@NCNTA, G/CoNi@NCNTAs and G/Ni@NCNTA composites were obtained after cooling to room temperature naturally.

Characterizations. The morphology and size of the synthesized samples were characterized by X-ray powder diffraction (XRD) using a X'Pert Pro diffractometer with Cu Kα radiation (λ=1.5418Å), scanning electron microscope (SEM) using a Hitachi SU8000, transmission electron microscope (TEM, JEM-2010, JEOL), X-ray photoelectron spectroscopy (XPS) were taken on X-ray photoelectron spectrometer (K-Alpha, Thermofisher Scienticfic Company) with Al Kα radiation generated at 12 kV and 150 W. Raman spectra were performed on a Raman spectrometer (Xplora Plus, Horiba Jobin Yvon Lab) using a 532 nm He−Ne laser. The pore diameter distribution and surface area were tested by nitrogen adsorption/desorption analysis (TRISTAR II3020). Brunauer−Emmett−Teller (BET) surface area and pore distribution employed on a Tristar II 3020 gas adsorption analyzer at 77 K. The magnetic property of samples was measured by a vibrating sample magnetometer (VSM; Lakeshore 7410) at room temperature.

Electromagnetic parameter measurement. The electromagnetic microwave absorption properties of the absorbing materials were measured by using a vector network analyzer (Anritsu MS4644A Vectorstar) in the 2−18 GHz range. The cylindrical sample (with the inner diameter and outer diameter are 3 mm and 7 mm respectively, and 3.0 mm thickness) was prepared by mixing absorbing materials with paraffin matrix was controlled to be 10 wt. %.
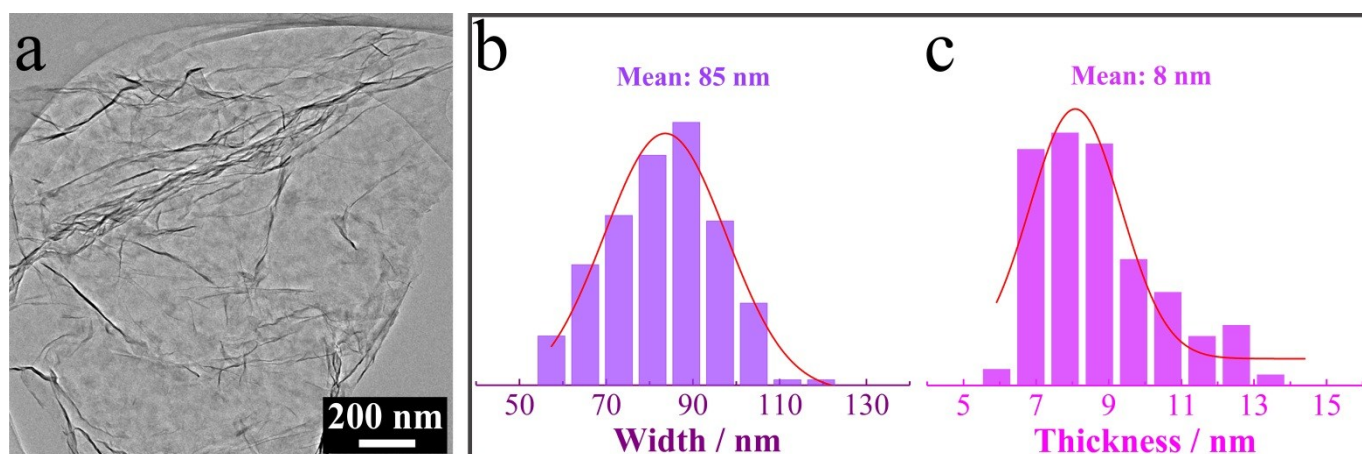
Fig. S1 TEM image (a), nanosheet width (b), and thickness (c) distributions of Co_1Ni_1-MOF/LDH in the G/Co_1Ni_1-MOF/LDH.
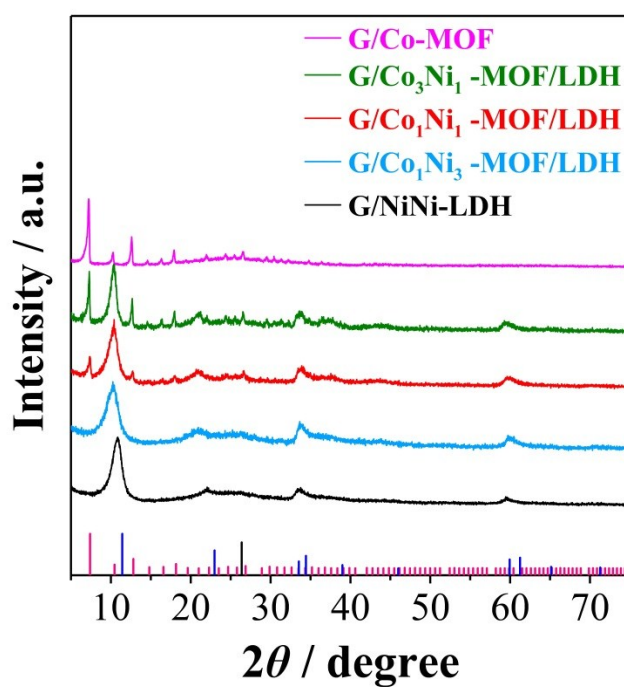
Fig. S2 XRD patterns of the G/Co-MOF, G/CoNi-MOF/LDHs and G/NiNi-LDH.
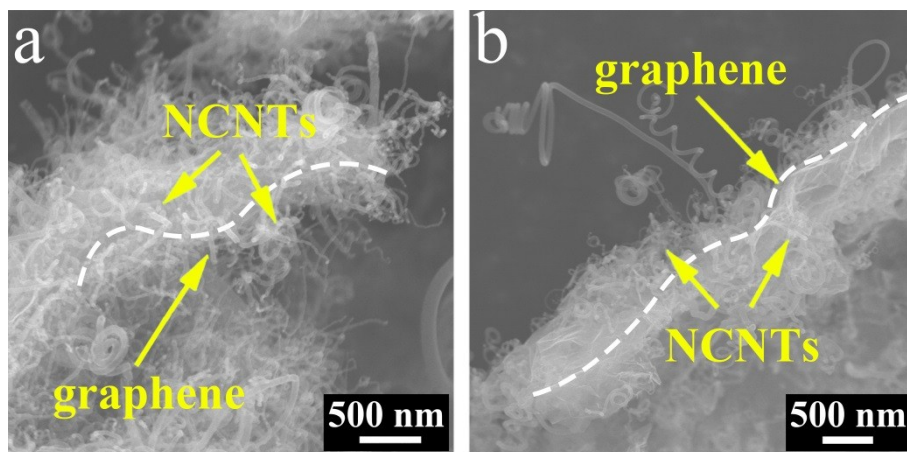
Fig. S3 SEM images of G/Co$_1$Ni$_1$@NCNTA.
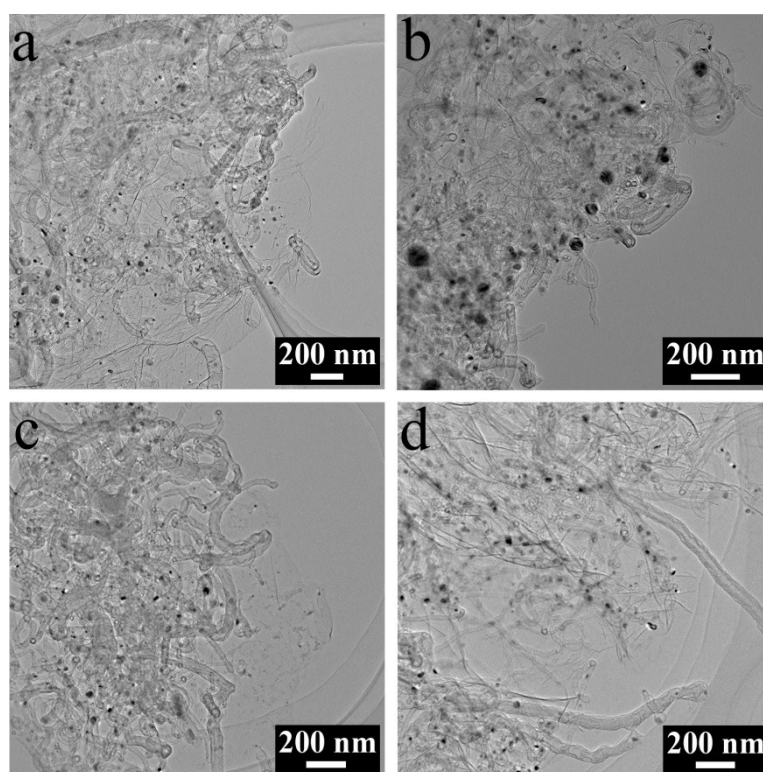
Fig. S4 TEM images of G/Co@NCNTA (a), G/Ni@NCNTA (b), G/Co$_3$Ni$_1$@NCNTA (c), and G/Co$_1$Ni$_3$@NCNTA (d).
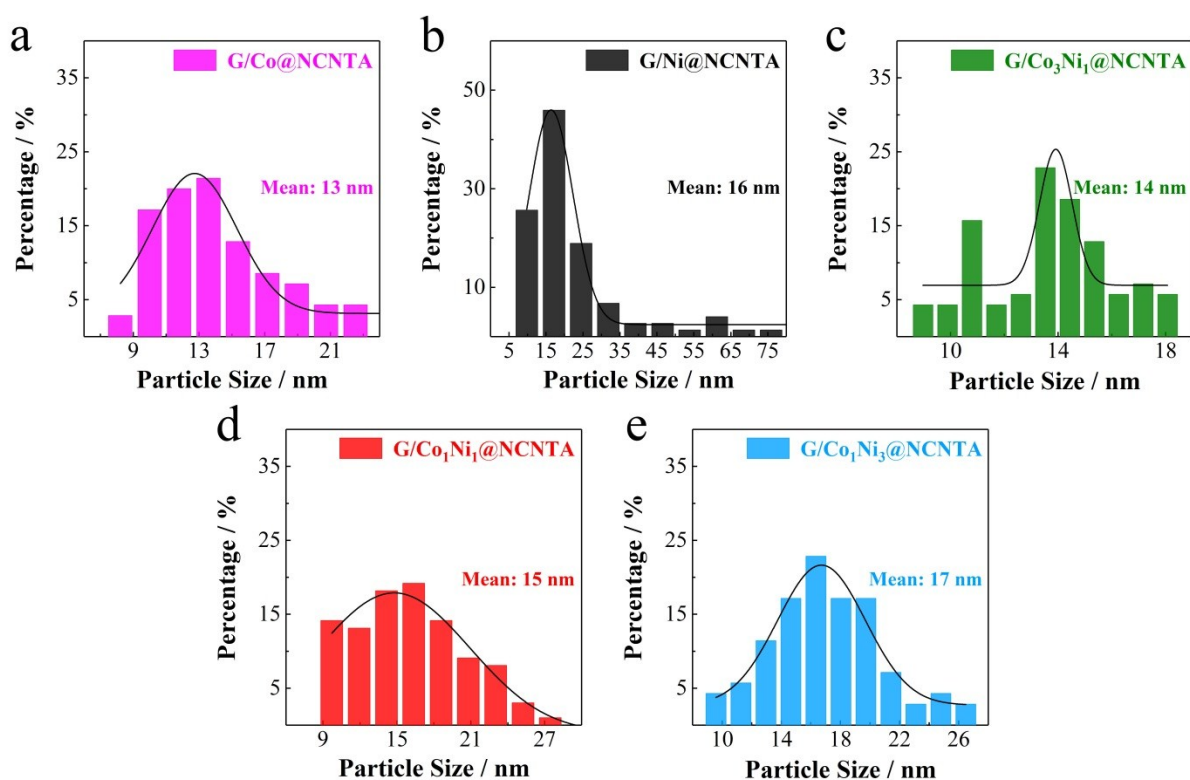
Fig. S5 The particle size distribution of metal NPs in the G/Co@NCNTA (a), G/Ni@NCNTA (b), G/Co$_3$Ni$_1$@NCNTA (c), G/Co$_1$Ni$_1$@NCNTA (d), and G/Co$_1$Ni$_3$@NCNTA (e).
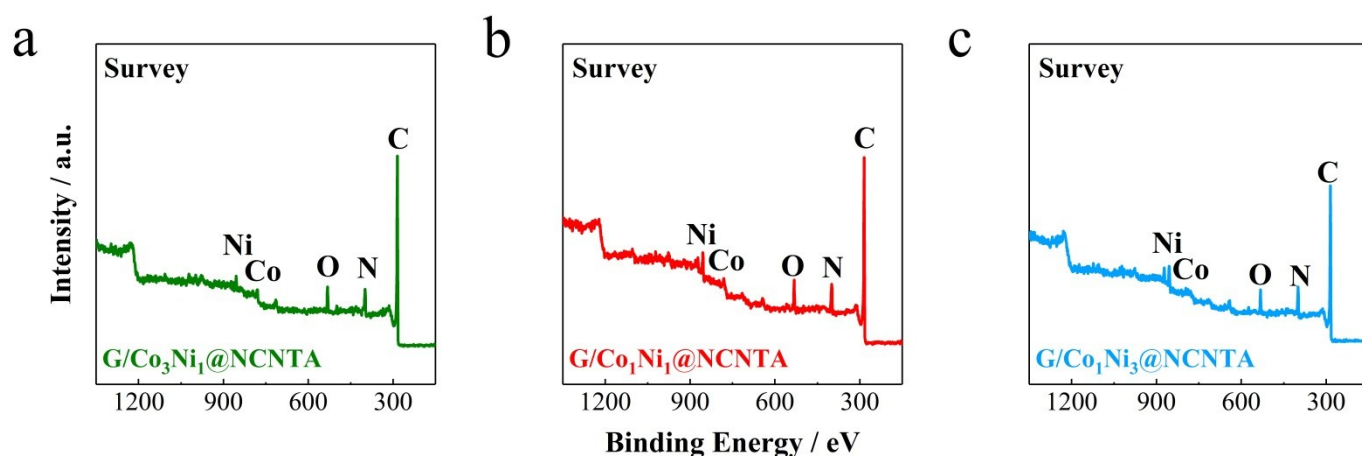
Fig. S6 XPS surveys of G/Co$_3$Ni$_1$@NCNTA (a), G/Co$_1$Ni$_1$@NCNTA (b), and G/Co$_1$Ni$_3$@NCNTA (c).
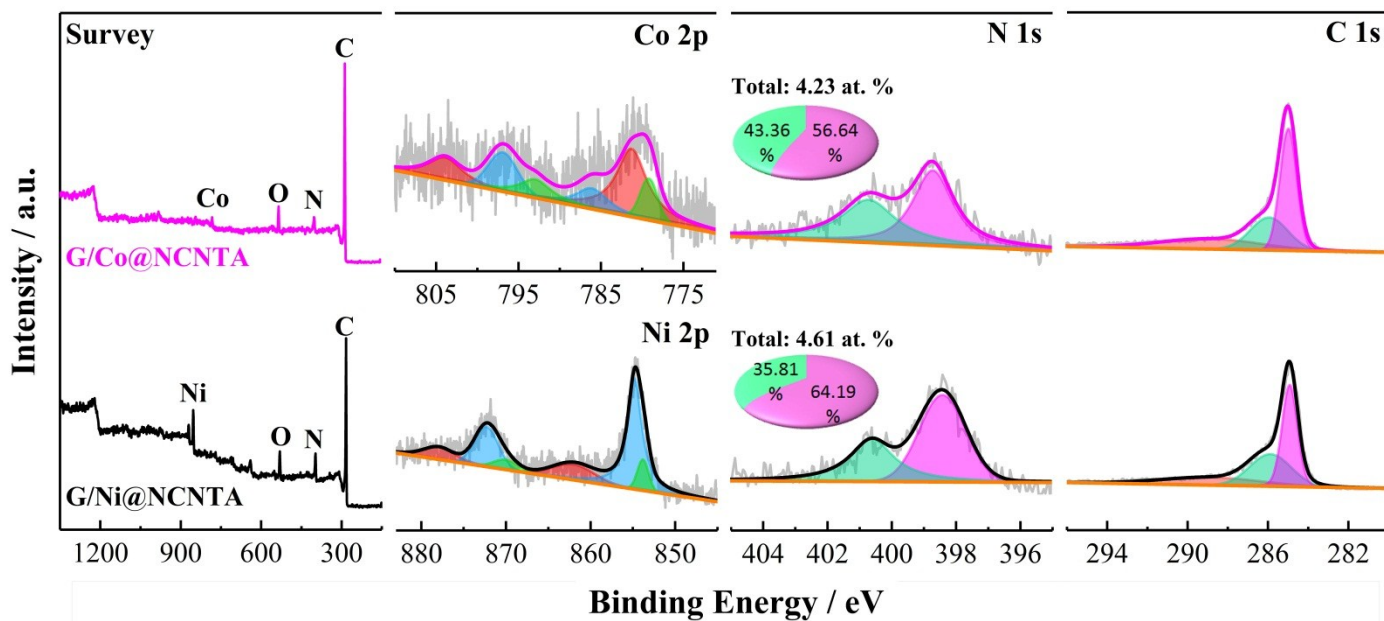
Fig. S7 XPS spectra of the G/Co@NCNTA and G/Ni@NCNTA.
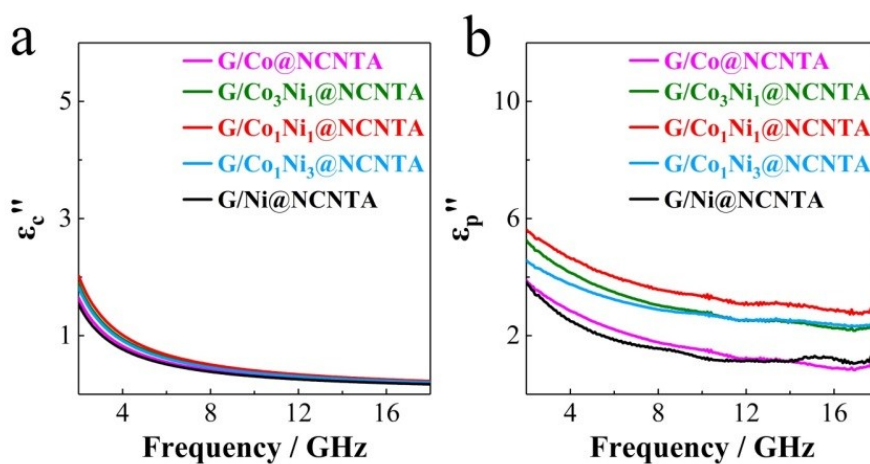
Fig. S8 The $\varepsilon_c'' - f$ (a) and $\varepsilon_p'' - f$ (b) curves of the 3D architectures.
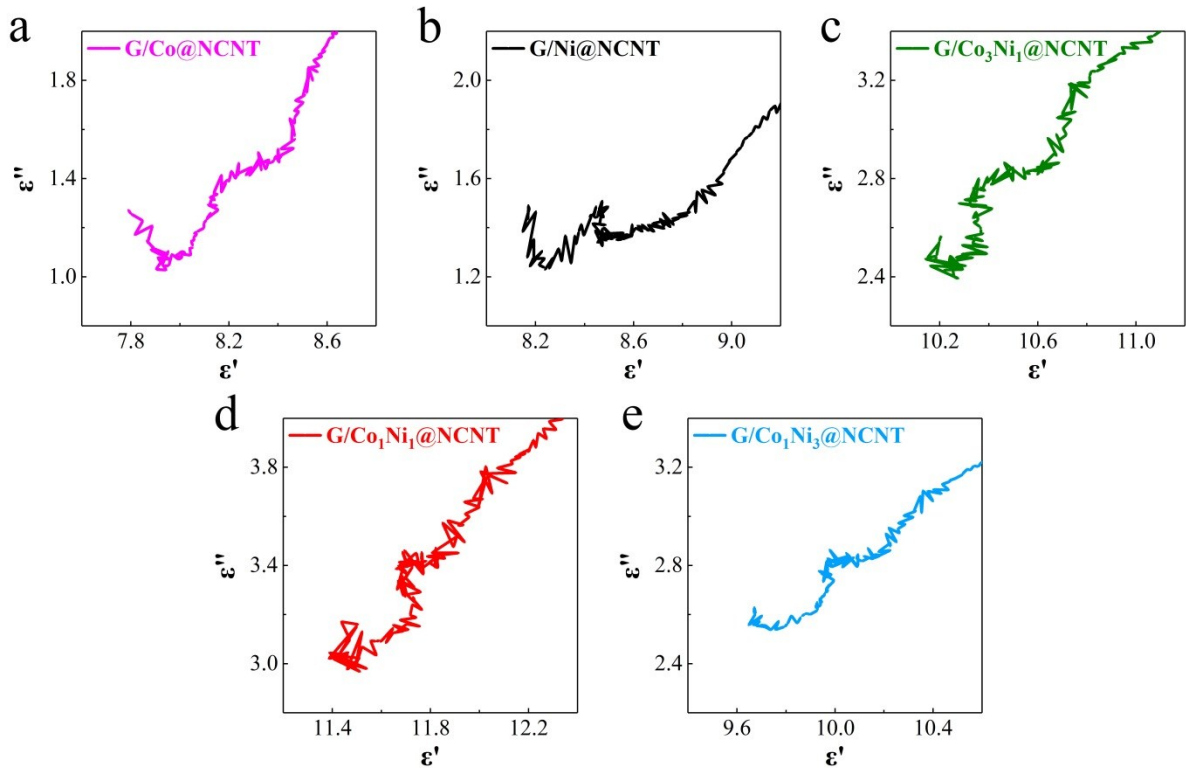
Fig. S9 The Cole – Cole semicircles of the 3D architectures.
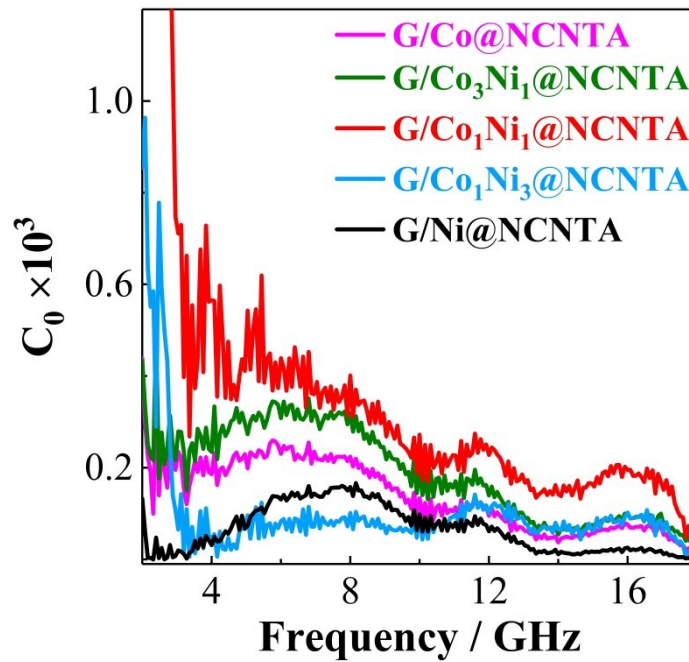
Fig. S10 The $C_0 - f$ curves of the 3D architectures.
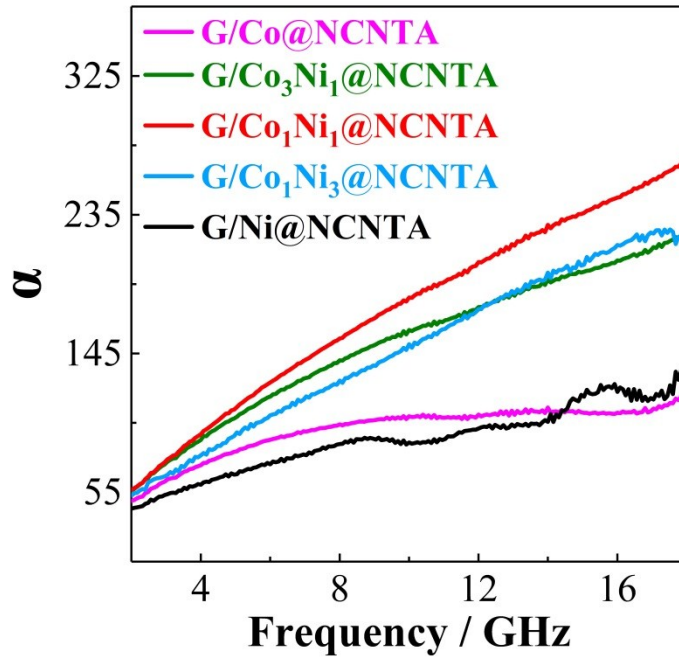
Fig. S11 The attenuation constant $\alpha - f$ curves of the 3D architectures.
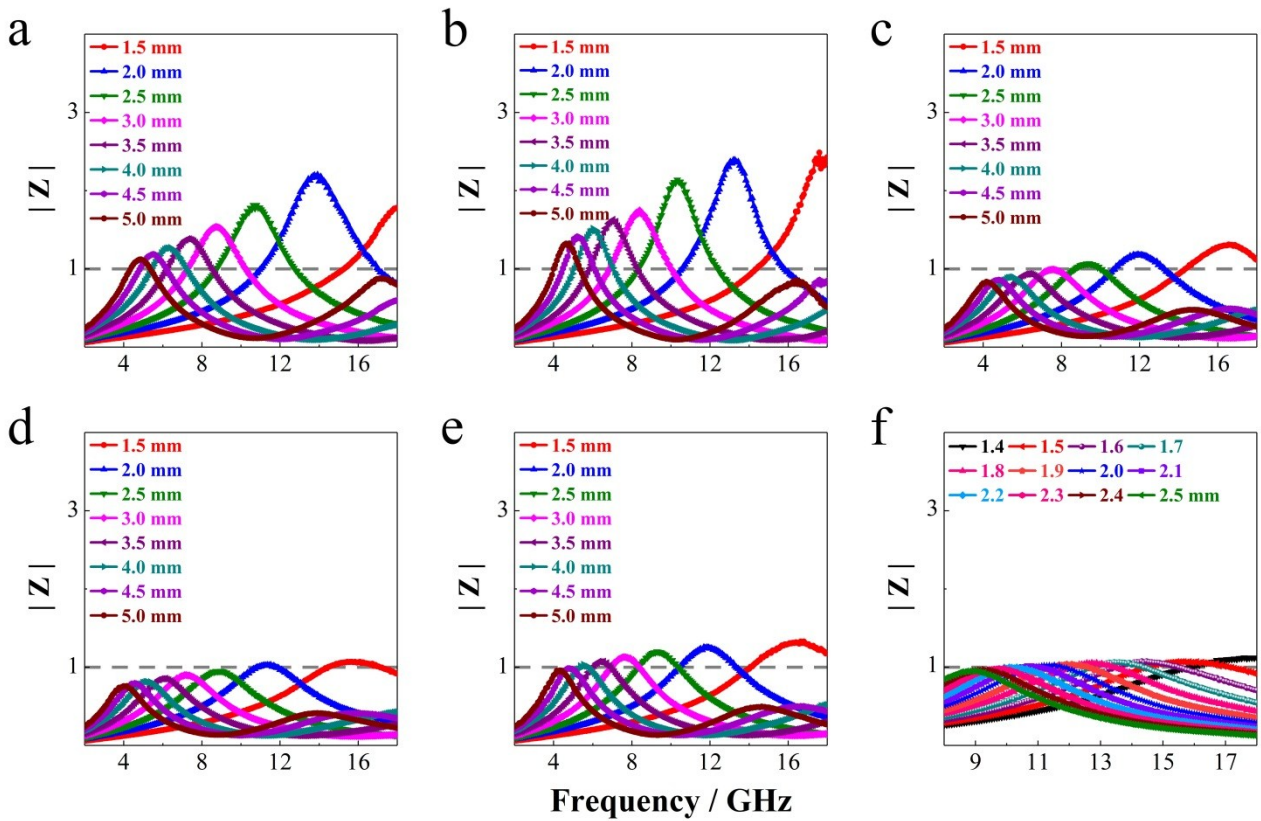
Fig. S12 The $|Z| - f$ curves of the G/Co@NCNTA (a), G/Ni@NCNTA (b), G/Co$_3$Ni$_1$@NCNTA (c), G/Co$_1$Ni$_1$@NCNTA (d), and G/Co$_1$Ni$_3$@NCNTA (e). The $|Z| - f$ curves of G/Co$_1$Ni$_1$@NCNTA at d of 1.4 − 2.5 mm (f).
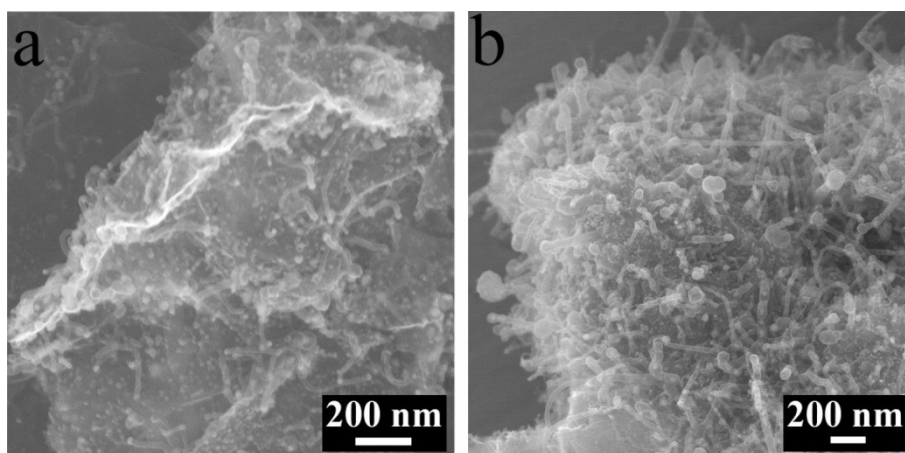
Fig. S13 SEM images of G/Co$_1$Ni$_1$@NCNTA-600 (a) and G/Co$_1$Ni$_1$@NCNTA-800 (b).
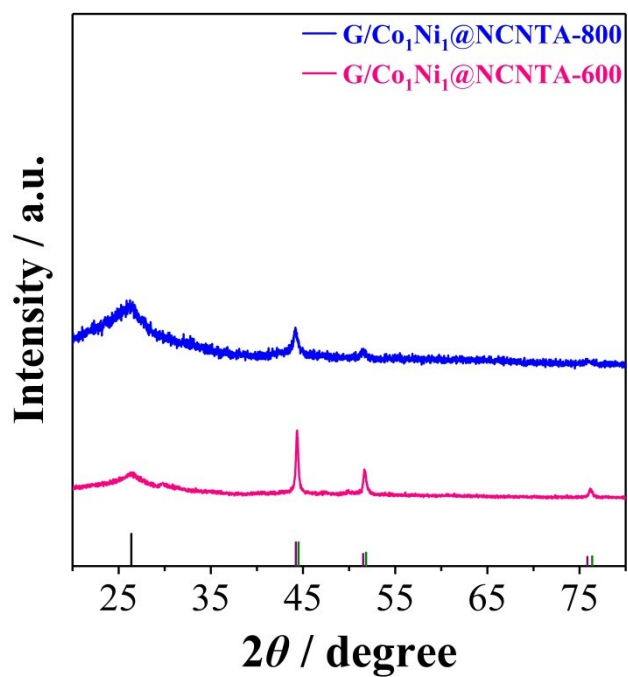
Fig. S14 XRD patterns of G/Co$_1$Ni$_1$@NCNTA-600 and G/Co$_1$Ni$_1$@NCNTA-800.
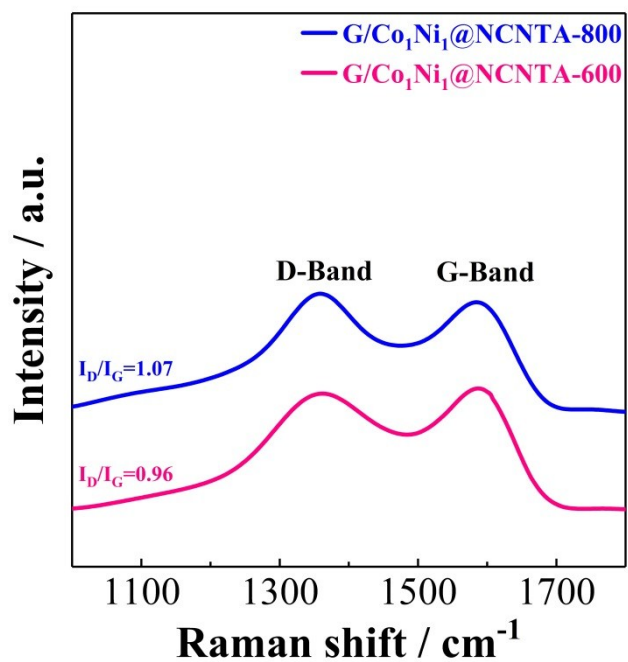
Fig. S15 Raman spectra of the G/Co$_1$Ni$_1$@NCNTA-600 and G/Co$_1$Ni$_1$@NCNTA-800.
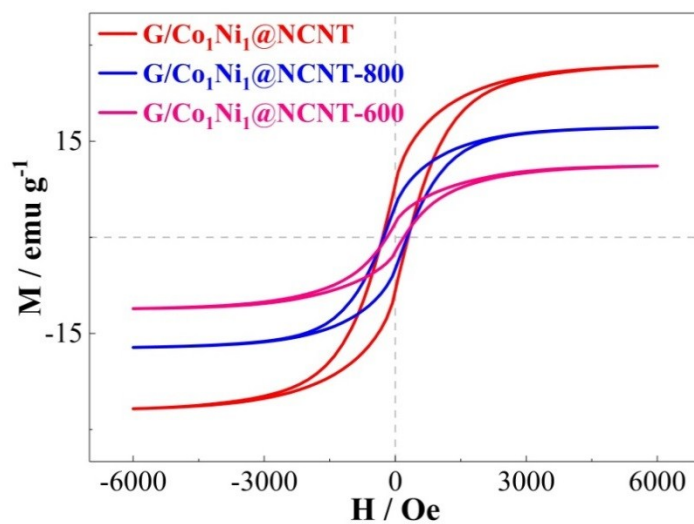
Fig. S16 Magnetization hysteresis loops of the G/Co$_1$Ni$_1$@NCNTA, G/Co$_1$Ni$_1$@NCNTA-600 and G/Co$_1$Ni$_1$@NCNTA-800.
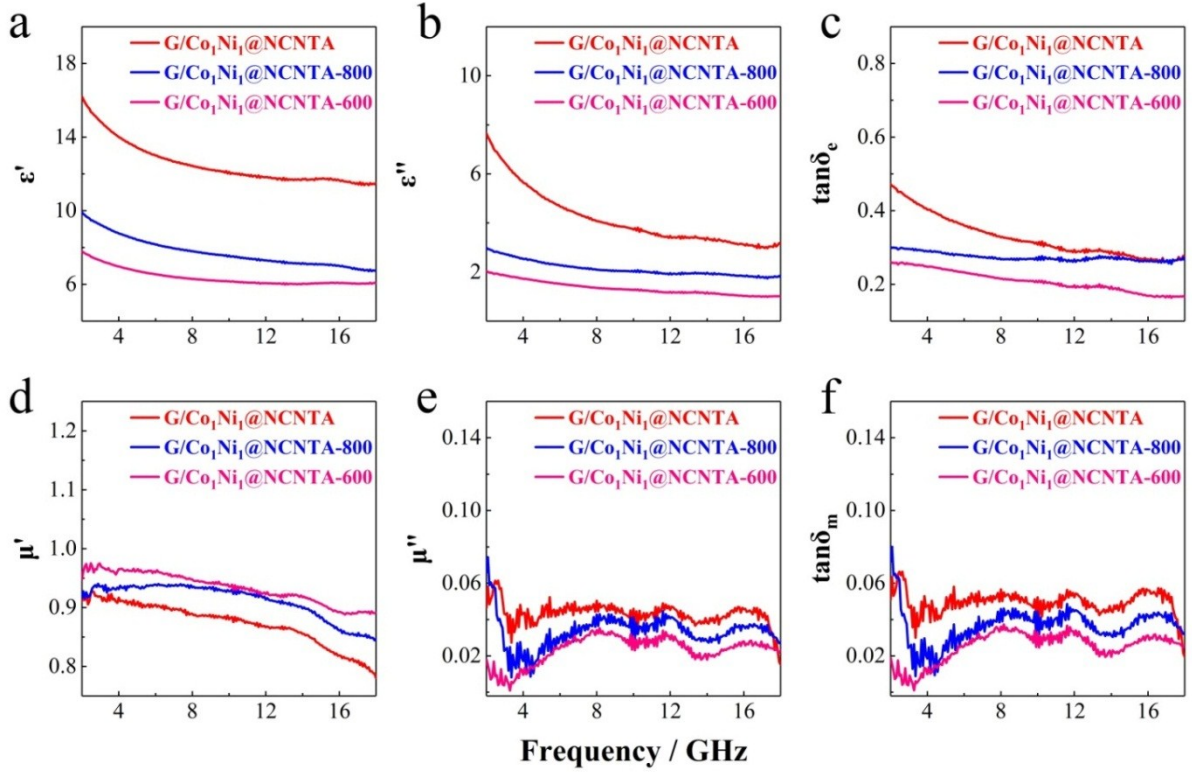
Fig. S17 The real parts of the relative complex permittivities (a), imaginary parts of the relative complex permittivities (b), and the dielectric loss tangents (c) of the $G/Co_1Ni_1@NCNTA$-600 and $G/Co_1Ni_1@NCNTA$-800. The real parts of the relative complex permeabilities (d), imaginary parts of the relative complex permeabilities (e), and the magnetic loss tangents (f) of the $G/Co_1Ni_1@NCNTA$, $G/Co_1Ni_1@NCNTA$-600 and $G/Co_1Ni_1@NCNTA$-800.
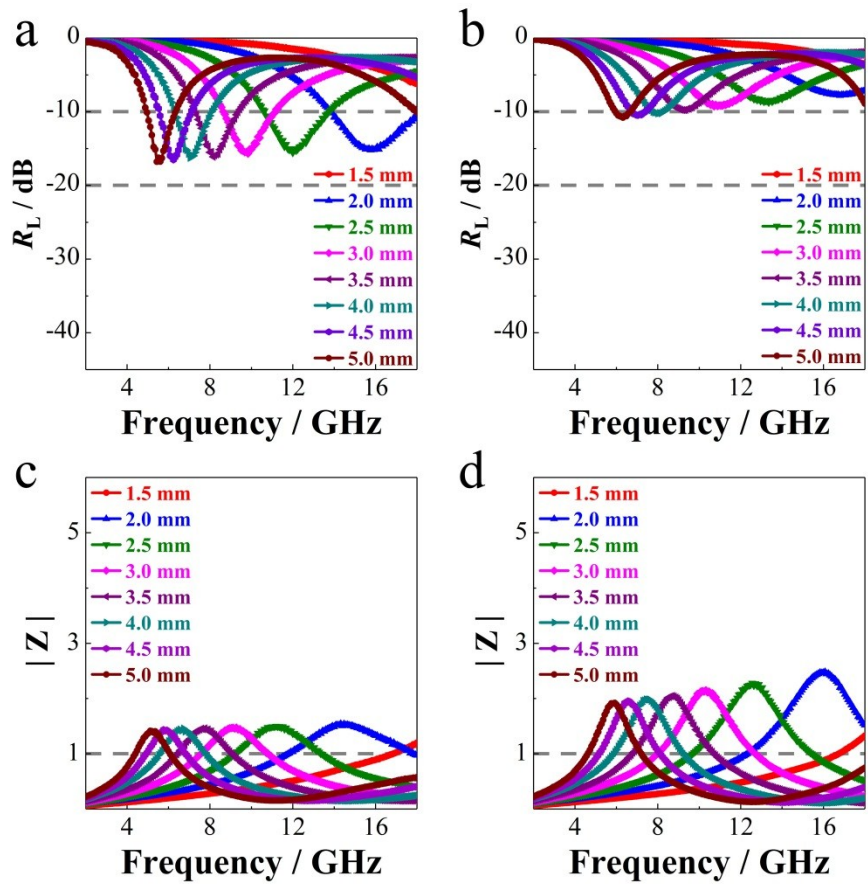
Fig. S18 The R_L data and the modulus of Z dependent on the frequency and the thickness of the absorbers for the G/Co$_1$Ni$_1$@NCNTA-800 (a, c), and G/Co$_1$Ni$_1$@NCNTA-600 (b, d).

Table S1 Detail comparison of the EME attenuation properties of the G/Co$_1$Ni$_1$@NCNTA to other reported materials.

Sample	$R_{L, min}$ / dB	Thickness / mm	Wt. %	EAB$_{10}$ / GHz	Ref.
NA$_2$ CA$_2$ CNT CNFs	-46.6	5.5	-	2.9	1
Fe/Fe$_3$C@NCNTs-600	-46	4.97	10	1.2	2
Fe$_x$C$_y$N$_z$/N-CNT	-25.1	4.0	12	1.3	3
Fe$_3$O$_4$/polypyrrole/CNT	-25.9	3.0	20	4.5	4
Co/N-doped carbon nanofibers	-25.7	2.0	5	4.3	5
MWCNTs/Fe	-39	4.27	60	1.43	6
MWCNTs/Co	-37	5.25	60	1.16	6
MWCNTs/Ni	-37	5.19	60	-	6
Fe$_2$O$_3$/G/CNTs	-45.8	3.0	40	3.7	7
CNT/RGO/BaFe$_{12}$O$_{19}$	-19.03	2.5	20	3.8	8
GO/CNT–Fe$_3$O$_4$	-37	5	30	2.1	9
rGO/AW900 C hybrid fiber	-35	5	-	2.4	10
Fe$_3$O$_4$/CNTs	-39.27	2	20	3.2	11
CNT@TiO$_2$	-31.8	2	30	3.1	12
Fe$_3$O$_4$/PANI@MWCNTs	-15.65	1.5	-	3.5	13
Carbon Nanotube@TiO$_2$	-31.8	2	30	2.76	12
Co−C/ MWCNTs	-48.9	2.99	15	3	14
NiCo$_2$/Graphene Nanosheets	-30	1.6	10	-	15
G/Co$_1$Ni$_1$@NCNTA	**-44.23**	2.0	**10**	3.32	herein
	-37.18	1.7	**10**	4.10	herein
	-37.52	**1.6**	**10**	**4.63**	herein

Notes and references

1. I. Abdalla, A. Salim, M. M. Zhu, J. Y. Yu, Z. L. Li and B. Ding, *ACS Appl. Mater. Interfaces*, 2018, **10**, 44561–44569.

2. Z. Xu, Y. C. Du, D. W. Liu, Y. H. Wang, W. J. Ma, Y. Wang, P. Xu and X. J. Han, *ACS Appl. Mater. Interfaces*, 2019, **11**, 4268–4277.

3. Y. L. Zhou, J. Miao, Y. H. Shen and A. J. Xie, *Appl. Surf. Sci.*, 2018, **453**, 83–92.

4. R. B. Yang, P. M. Reddy, C. J. Chang, P. A. Chen, J. K. Chen and C. C. Chang, *Chem. Eng. J.*, 2016, **285**, 497–507.

5. H. H. Liu, Y. J. Li, M. W. Yuan, G. B. Sun, H. F. Li, S. L. Ma, Q. L. Liao and Y. Zhang, *ACS Appl. Mater. Interfaces*, 2018, **10**, 22591–22601.

6. F. S. Wen, F. Zhang and Z. y. Liu, *J Phys. Chem. C*, 2011, **115**, 14025–14030.

7. N. Zhou, Q. D. An, Z. Y. Xiao, S. R. Zhai and Z. Shi, *RSC Adv.*, 2017, **7**, 45156–45169.

8. T. K. Zhao, X. L. Ji, W. B. Jin, C. Wang, W. X. Ma, J. J. Gao, A. Dang, T. H. Li, S. M. Shang and Z. F. Zhou, *RSC Adv.*, 2017, **7**, 15903–15910.

9. L. N. Wang, X. L. Jia, Y. F. Li, F. Yang, L. Q. Zhang, L. P. Liu, X. Ren and H. T. Yang, *J. Mater. Chem. A*, 2014, **2**, 14940–14946.

10. D. Estevez, F. X. Qin, L. Quan, Y. Luo, X. F. Zheng, H. Wang and H. X. Peng, *Carbon*, 2018, **132**, 486–494.

11. S. Y. Liu, L. F. Mei, X. L. Liang, L. B. Liao, G. C. Lv, S. F. Ma, S. Y. Lu, A. Abdelkader and K. Xi, *ACS Appl. Mater. Interfaces*, 2018, **10**, 29467–29475.

12. Z. C. Mo, R. L. Yang, D. W. Lu, L. L. Yang, Q. M. Hu, H. B. Li, H. Zhu, Z. K. Tang and X. C. Gui, *Carbon*, 2019, **144**, 433–439.

13. Y. H. Zhao, Z. Zhou, G. X. Chen and Q. F. Li, *Mater. Lett.*, 2018, **233**, 203–206.

14. Y. C. Yin, X. F. Liu, X. J. Wei, Y. Li, X. Y. Nie, R. H. Yu and J. L. Shui, *ACS Appl. Mater. Interfaces*, 2017, **9**, 30850–30861.

15. R. L. Yang, B. C. Wang, J. Y. Xiang, C. P. Mu, C. Zhang, F. S. Wen, C. Wang, C. Su and Z. Y. Liu, *ACS Appl. Mater. Interfaces*, 2017, **9**, 12673–12679.